DEVELOPMENT OF A CARBON/EPOXY COMPOSITE NOZZLE MANUFACTURED BY FILAMENT WINDING

Dalibor I.H.[1], Almeida Jr. J.H.S.[1], Shynkarenko O.[2], Amico S.C.[1]

[1]LAPOL/GCOMP/UFRGS, Porto Alegre/RS, Brazil
Email: ihd.dal@gmail.com; jhsajunior@globomail.com; amico@ufrgs.br
[2]LAICA/UnB, Brasília/DF, Brazil
Email: olexiy@unb.br

Keywords: Composite nozzle, winding trajectory, filament winding.

Abstract

The subject of this development is a linerless nozzle manufactured by filament winding process with prepreg carbon fiber. The nozzle will be assembled on a hybrid rocket motor planned by Brazilian Space Agency - AEB in the SARA project, to desecelerate a low orbital satellite in the reentry to the atmosphere. The nozzle during ignition time of about 12s is submitted to inner pressure, axial force, erosion and high temperature. The development consists of structural analysis, the lay up definition, the determination of process variables and the manufacturing by filament winding process in which process variables were simulated with specific CAD-CAM software. Due to the bell shaped inner surface of the nozzle, a high slippage tendency occurs during winding and restricted the winding angle alternatives. To withstand high temperature a special coating were developed and applied directly on the mandrel before the winding procedure. Partial tests showed the viability to manufacture the nozzle with prepreg carbon fiber and epoxy matrix by the filament winding process.

1. Introduction

Hybrid rocket propulsion systems use solid fuel and liquid or gaseous oxidizers and are safer than conventional systems with solid or liquid propelled motors. In the ignition, gasification of the solid propellant occurs, which oxidizes with the vapor of the oxidizer, generating hot gases, which flow through the nozzle. The thrust on the rocket motor occurs due to the change of momentum of the ejected matter at supersonic speed. The nozzle accelerates with the expansion rate given by the ratio of the exit area and the area at the throat section and leads the gaseous matter burned in the combustion chamber to expand in the nozzle. Figure 1 shows a draft from a rocket motor in which arrows indicate the pressure variation inside and outside the engine. The nozzle has a converging and a diverging section and between the throat with the smallest area. The flow has supersonic speed in the diverging nozzle section. At the throat section, the flow turns from subsonic to supersonic. At the exit cross-section of the nozzle the pressure has to be the same as outside atmospheric pressure for the maximum motor efficiency. However, as the rocket passes through different altitudes with different atmospheric pressures, only at one altitude the inner pressure is ideal. If atmospheric pressure is higher, an overexpansion will occur and thrust decreases. The nozzle can be submitted to erosion due to the hot matter at high velocity and high temperature flow. The transformation of thermal to kinetic energy is assumed to be reversible in region far from the wall boundary layer and shockwaves. Nevertheless, in the nozzle wall the flow is non-isentropic. The surface quality of the material has influence to the structure of the boundary layer and parameters of turbulence. High roughness of the surface compared

Excerpt from ISBN 978-3-00-053387-7

with the displacement thickness in boundary layer can also cause disturbances inside the supersonic flow. These disturbances are weak or strong shockwaves, supported with the flow separation regions and micro-vortexes inside the boundary layer. If these protuberances happen, the speed of outgoing matter decreases and the temperature increases. In this way an overheating may occur. So, a smooth inner surface is required for the efficient propulsion process. Nozzles may be fixed, movable, submerged, and extendible or blast tube mounted (1,2).

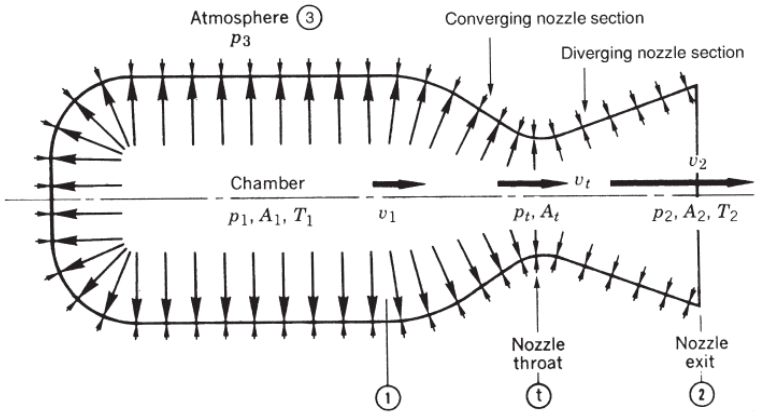

Figure 1- Rocket motor combustion chamber with nozzle [2].

Nozzles may be manufactured with steel, keramic or composite materials allways considering above mentioned restrictions, as smoth internal surface with high temperature resistence.

2. Filament winding process

Among several processes for composite materials, filament winding - FW may take full advantage of fibers properties and it is increasingly used to manufacture parts in which high relation strength/weight is required, as in the aerospace industry. In the process, impregnated fibers are wound over a mandrel in a regular repetitive way so that a mosaic pattern with diamond shape is formed. One complete circuit is compound of 2 strokes, in the first one, the tow is wound toward the right end and then in the returning course the tow is wound toward the left end (or vice versa). As in all composite materials, the fiber direction is the most important variable, which provides the strength to the material. In FW the fiber direction is defined trough the winding angle, which is positive in one stroke and negative in the returning one. The trajectory performed by the fiber over the mandrel may be geodesic or non-geodesic. The geodesic path is the natural trajectory over a mandrel when there is no friction between tow and mandrel [3]. A deviation from the geodesic path is only possible with a friction coefficient, the higher the friction the higher the possible deviation. The Clairaut relation determines the geodesic path over a revolution surface as follows:

$$r sen\alpha = c \tag{1}$$

where r is the parallel radius, α the winding angle and c a constant. The constant c may be obtained with the initial angle and respective radius. When the winding angle achieves 90° it will be iqual to the local radius. This is an inflexion point from which the tow begins the returnig way.

The non-geosecid trajectory is defined by:

$$\frac{d\alpha}{dz} = \lambda\left[\frac{sen\alpha.tg\alpha}{r} - \frac{r^{''}.cos\alpha}{1+r'^2}\right] - \frac{r'}{r}tg\alpha \tag{2}$$

Excerpt from ISBN 978-3-00-053387-7

where $d\alpha/dz$ is the variation of the winding angle as function of the axial coordinate, r is the parallel radius defined by the Eq. of the revolution surface and r' the first derivative of this Eq. and λ the slippage coefficient. When the slippage coefficient is equal to zero, there is no friction between the fiber and the mandrel, the fiber path will be geodesic. In this case the solution of the differential Eq. (Eq.2) is the Clairaut relation (Eq.1). When $\lambda \neq 0$ there is no analytical solution of the differential Eq. (Eq.2) and a numerical method, like Euler, Heun or Runge Kutta must be applied [4]. At the point where the winding angle is iqual 90° there is no mathematical solution and approximations procedure may be applied. The wall thickness formed in the FW process changes with the mandrel diameter and winding angle as:

$$t(r) = \frac{r_c cos\alpha_c}{r cos\alpha} t_c \tag{3}$$

where t_c is thickness for the largest diameter.

Each wound surface has a non-geodesic path in the region where the fiber changes the direction. The minimum length for the returning region is defined by:

$$l_e = \frac{R}{f}\left(\frac{1}{sin\alpha} - 1\right) \tag{4}$$

where R is the radius and f the friction coefficient.
Considering a shell of revolution under internal pressure the equilibrium Eq.s are [5,6]:

$$\frac{N_m}{r_m} + \frac{N_p}{r_p} = p \tag{5}$$

$$N_m = \frac{pr\sqrt{1+r'^2}}{2} \tag{6}$$

$$N_p = \frac{pr\sqrt{1+r'^2}}{2}\left(2 + \frac{rr''}{1+r'^2}\right) \tag{7}$$

where N_m and N_p are the principal stresses per unit length, respectively, meridional and circumferential, and r_m and r_p are the meridional and circumferential radii of the revolution surface and p the internal pressure. The parameters r_m and r_p are calculated by the inverse of the curvatures k_m and k_p . The optimal winding angle will be obtained when meridional and circunferential stresses are the same which is obtained by:

$$\alpha = arctg\sqrt{\frac{N_p}{N_m}} \tag{8}$$

The curvatures are obtained by:

$$k_m = \frac{e}{E} = -\frac{r''}{[1+r'^2]^{\frac{3}{2}}} \tag{9}$$

$$k_p = \frac{g}{G} = \frac{1}{r\sqrt{1+r'^2}} \tag{10}$$

where E, G, e and g are, respectively, the first and second fundamental magnitudes of a revolution surface.

3. Materials and Methods

The nozzle, with only the diverging section, subject of this research, is shown in Figure 2. The surface is defined through:

Excerpt from ISBN 978-3-00-053387-7

$$r = 17{,}9 + 0{,}480329.x - 0{,}00226208.x^2 + 5{,}5731.10^{-6}.x^3 \quad (11)$$

where *r(x)* is the radius.

Only the diverging section will be manufactured as the converging section is part of the moto case. During ignition time (about 12 s), the nozzle will be submitted to an internal pressure of 30 bar and temperature of about 1200 °C. The axial force may be disconsidered.

The winding equipment consists of a robot from Kuka with 7 degrees of freedom. The filament winding devices as tow supply, until 4 simultaneously, individual tow tension control and spindle with chucks for the mandrel rotation were from MFtech. Maximal mandrel length is 4 m and maximal diameter 1,5 m. The equipment is prepared only for dry winding, it means, there is no impregnation device. The software CadWind enables an off equipment programming and performs Cad/Cam. After winding, curing occurs in an oven at a temperature of 130 °C during 4 h.

The towpreg is T700 from TCR Composites which are carbon filaments pre-impregnated with an UF3369 epoxi matrix.

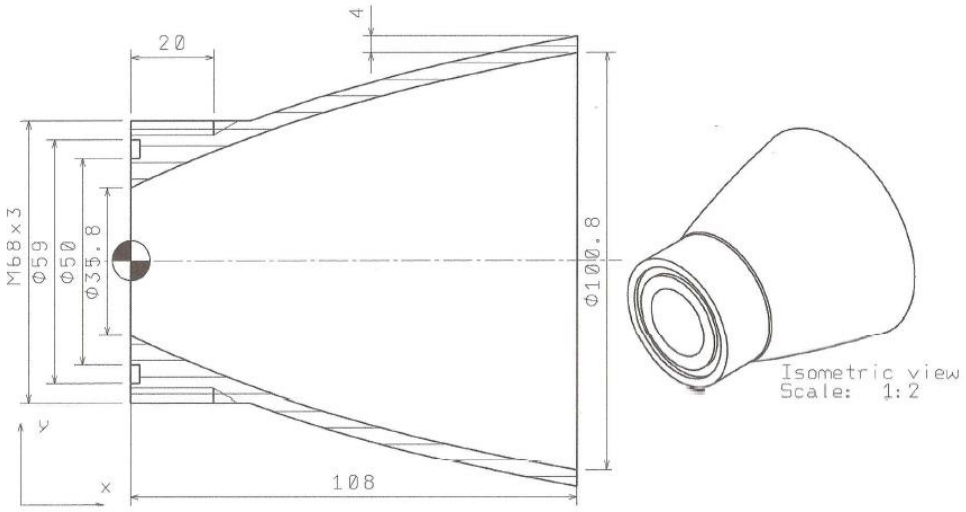

Figure 2- Design of the composite nozzle.

Table 1 shows material properties used to manufacture the composite nozzles [7].

Table 1-Caracterization of the carbon/epoxy laminate.

Property		Test	Property		Test
Longitudinal elastic modulus tensile / compressive (GPa)	E_{t1}/E_{c1}	153	Shear strength (MPa)	τ_{12}	76.7
Transversal elastic modulus tensile / compressive (GPa)	E_{t2}/E_{c2}	12.2	Fiber volume fraction	V_f	0.71
In plane shear modulus (GPa)	G_{12}	5.9	Fiber thickness (mm)		0,2
Major Poisson ratio	v_{12}	0.34	Tow width (mm)		2
Minor Poisson ratio	v_{21}	0.029	Tow weight tex (g/1000m)		
Longitudinal tensile strength (MPa)	S_{t1}	1822	Density fiber g/cm3		
Transversal strength tensile (MPa)	S_{t2}	63.2	Density resin g/cm3		
Longitudinal strength compressive (MPa)	S_{c1}	840	Diameter filaments μm		7.1
Transversal strength compressive (MPa)	S_{c2}	153			

Excerpt from ISBN 978-3-00-053387-7

4. Results

Structural analysis begins with Eq.s (Eq. 9) and (Eq. 10) to calculate principal curvatures whose inverses are the principal radii. Through Eq.s (Eq. 5), (Eq. 6) and (Eq. 7), the principal stresses are calculated as shown in Figure 3.

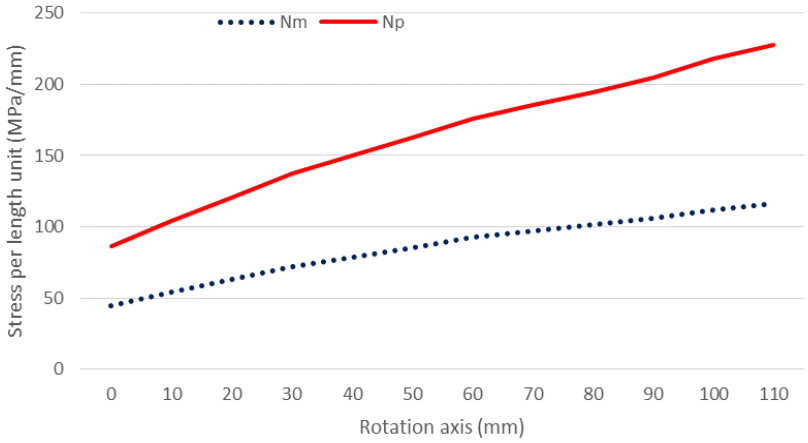

Figure 3 -Principal stresses.

The winding angle showed in Figure 4 is obtained by Eq. 8 for the stresses showed in Figure 3.

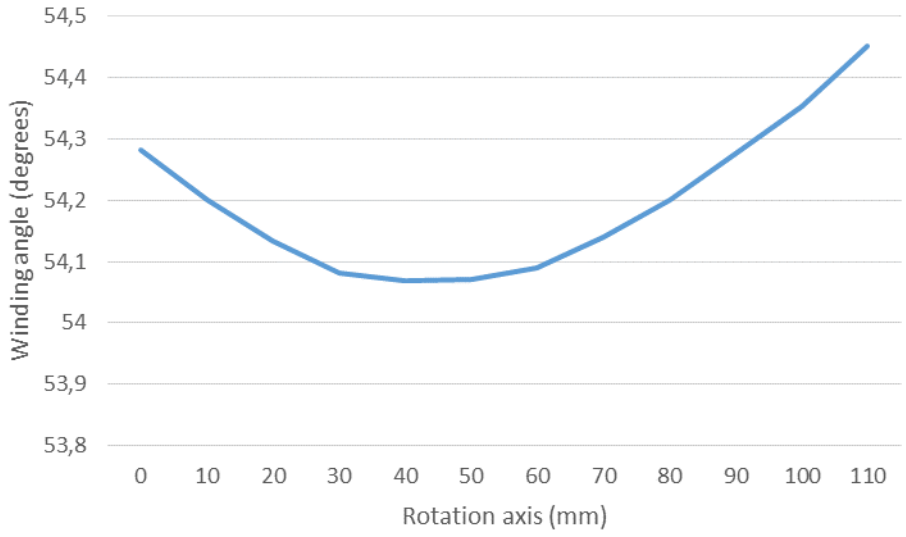

Figure 4 - Winding angle as an optimal relation between the principal stresses.

Thickness as Eq. (Eq. 3) and winding angle as Eq. (Eq. 1) are shown in Figure 5. The winding angle of 20° on the largest diameter (z=108 mm) is the largest angle with which a full geodesic path is fullfilled. It means, taking an angle larger than 20° the path will not reach the other side of the nozzle (z=0). This happens because the path achieves the winding angle of

Excerpt from ISBN 978-3-00-053387-7

90° when z >0. A smaller angle than 20° is possible, as example an angle of 17° on the largest diameter (z=108mm) will give an angle of 56° on the smallest diameter (z=0).

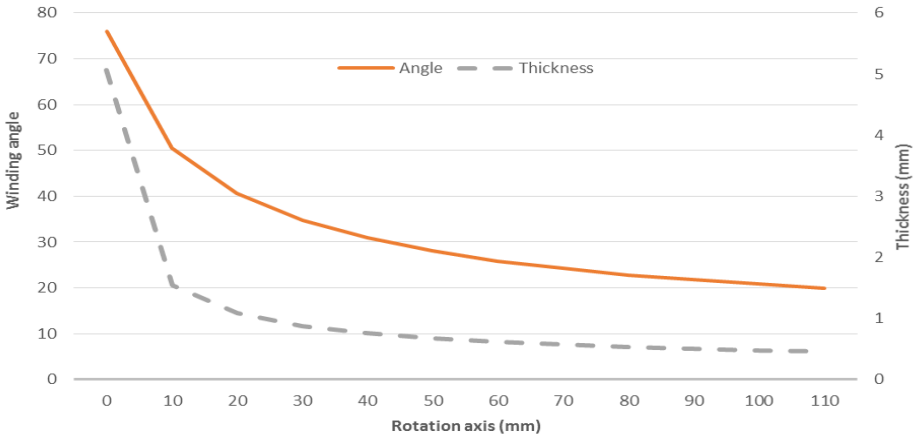

Figure 5- Thickness and winding angle.

Since a geodesic path with a winding angle near to 54° is not possible, a solution has to be found with non-geodesic trajectories. In this research the determination of process variables for a non geodesic winding was performed only with the above mentioned software. Several options were analysed and finally a non geodesic path with following variables was selected: winding angle (on largest diameter): 50°; friction factor: 0.4; pattern: 8/1. Through netting analysis, it was obtained that two layers provide sufficient resistance to the composite structure when only under internal pressure. To guarantee a suitable friction and provide fire resistance, the mandrel was coated with a special gelcoat prepared with phenolic resin, silicate oxid, epoxi and a ceramic component. First flammable tests showed that the coating resist high temperature (about 1100 °C) until 20 s before burn.

The mandrel is designed with a cylindrical extension in accordance with the returning length obtained with the Eq. 4 and displayed in Figure 6.

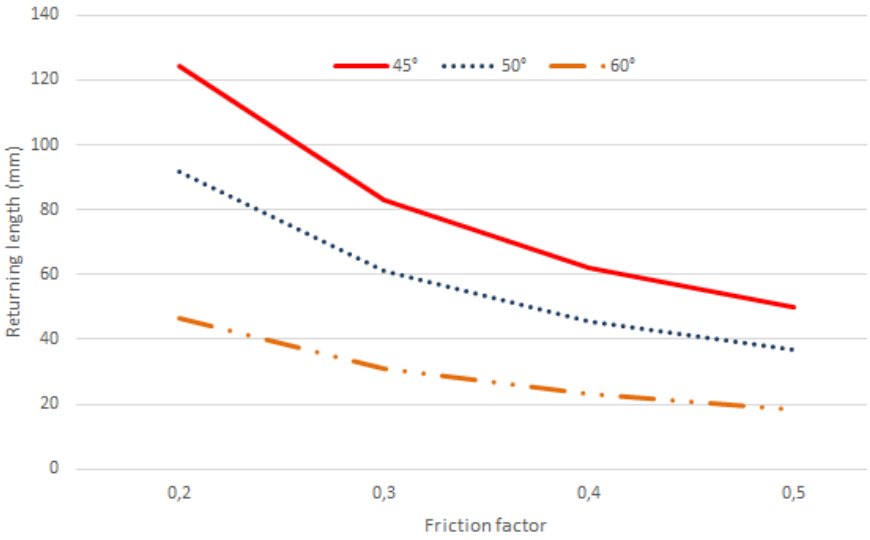

Figure 6 - Returning length as function of winding angles of 45°, 50° and 60°.

Excerpt from ISBN 978-3-00-053387-7

5. Discussion and conclusions

According membrane theory the principal stresses, in meridional and parallel direction, considering only internal pressure, were obtained for the nozzle. To withstand this load, optimal winding angle is calculated through the stress relation in Eq. 8. The optimal winding angle varies near to 54°, similar to the optimal angle on a cilyndrical surface (54.7°). Due to the characteristics of the filament winding process the winding angle and thickness change according the surface of the nozzle. The geodesic path, as the natural trajectory when there is no friction between tow and mandrel, is easy to accomplish for cylindrical surfaces. Also for conical surfaces, because on the surface of the developed cone the geodesic path is a straight line. But, on conical surfaces and other revolution surfaces, the winding procedure generates a changing thickness which is function of the parallel radius and the local winding angle. In this research is shown that on a surface defined trough a polynomial Eq., as from this nozzle, the possible winding angles are limited and the, normally preferable, geodesic path cannot be applied. The maximum possible winding angle is 20° to complete the winding. Therefore, applying the specific CAD/CAM software, a non geodesic trajectory was selected and the mandrel was designed with a cylindrical extension according Eq. 4. At the same time, a special gelcoat was developed to withstand high temperatures.

The nozzle manufactured by filament winding is shown in Figure 7. The solution presented in the figure below for the the thread is the separated machining and gluing on the composite part. This alternative indeed, has not been tested.

Figure 7 - The manufactured composite nozzle.

6. References

[1] Shynkarenko O., Andrianov A., Bertoldi A.E. Low- thrust hybrid motor efficiency research for design optimization purposes. Propulsion and energy forum. 51st AIAA/SAE/ASEE Joint propulsion conference. Orlando USA. 2015.
[2] Sutton, G., Biblarz, O. Rocket Propulsion Elements. 8th. John Wiley & Sons. 2010.
[3] Zu L., He Q., Shi J., Li H. Non geodesic trajectories for filament wound composite truncated conical domes. Applied mechanics and materials 281.2013.
[4] Kreyszig E. Advanced engineering mathematics. John Wiley & Sons. 2011.
[5] Koussios S. Filament winding-a unified approach. Phd thesis. Technische Universität Delft.2004.
[6] Vasiliev, V. Composite Pressure Vessels. Analysis, Design and Manufacturing. Bull Ridge Publishing.2009.
[7] Almeida Júnior J.H.S., Souza S.D., Botelho E.C., Amico S.C. Carbon fiber reinforced epoxy filament wound composite laminates exposed to hygrothermal conditioning. Journal of Materials Science, v. 51, n.9, p. 4697-4708, 2016.

Excerpt from ISBN 978-3-00-053387-7